

AperTO - Archivio Istituzionale Open Access dell'Università di Torino

Hades experiments: investigation of hadron in-medium properties

This is the author's manuscript

Original Citation:

Availability:

This version is available <http://hdl.handle.net/2318/146156> since

Published version:

DOI:10.1088/1742-6596/420/1/012013

Terms of use:

Open Access

Anyone can freely access the full text of works made available as "Open Access". Works made available under a Creative Commons license can be used according to the terms and conditions of said license. Use of all other works requires consent of the right holder (author or publisher) if not exempted from copyright protection by the applicable law.

(Article begins on next page)

Hades experiments: investigation of hadron in-medium properties

This content has been downloaded from IOPscience. Please scroll down to see the full text.

2013 J. Phys.: Conf. Ser. 420 012013

(<http://iopscience.iop.org/1742-6596/420/1/012013>)

View [the table of contents for this issue](#), or go to the [journal homepage](#) for more

Download details:

IP Address: 90.147.27.47

This content was downloaded on 16/06/2014 at 14:15

Please note that [terms and conditions apply](#).

Hades experiments: investigation of hadron in-medium properties

Piotr Salabura

M.Smoluchowski Institute of Physics Jagiellonian University, 30-052 Krakw, Poland

E-mail: piotr.salabura@uj.edu.pl

for the HADES collaboration

G. Agakishiev⁶, C. Behnke⁷, D. Belver¹⁶, A. Belyaev⁶,
 J.C. Berger-Chen⁸, A. Blanco¹, C. Blume⁷, M. Böhmer⁹,
 P. Cabanelas¹⁶, S. Chernenko⁶, C. Driisa¹⁰, A. Dybczak², E. Epple⁸,
 L. Fabbietti⁸, O. Fateev⁶, P. Fonte^{1,a}, J. Friese⁹, I. Fröhlich⁷,
 T. Galatyuk^{4,b}, J. A. Garzón¹⁶, K. Gill⁷, M. Golubeva¹¹,
 D. González-Díaz⁴, F. Guber¹¹, M. Gumberidze¹⁴, S. Harabasz^{4,2},
 T. Hennino¹⁴, R. Holzmann³, P. Huck⁹, C. Höhne¹⁰, A. Ierusalimov⁶,
 A. Ivashkin¹¹, M. Jurkovic⁹, B. Kämpfer^{5,c}, T. Karavicheva¹¹,
 I. Koenig³, W. Koenig³, B. W. Kolb³, G. Korcyl², G. Kornakov¹⁶,
 R. Kotte⁵, A. Krása¹⁵, E. Krebs⁷, F. Krizek¹⁵, H. Kuc^{2,14},
 A. Kugler¹⁵, A. Kurepin¹¹, A. Kurilkin⁶, P. Kurilkin⁶, V. Ladygin⁶,
 R. Lalik⁸, S. Lang³, K. Lapidus⁸, A. Lebedev¹², L. Lopes¹,
 M. Lorenz⁷, L. Maier⁹, A. Mangiarotti¹, J. Markert⁷, V. Metag¹⁰,
 J. Michel⁷, C. Müntz⁷, R. Münzer⁸, L. Naumann⁵, M. Palka²,
 Y. Parpottas^{13,d}, V. Pechenov³, O. Pechenova⁷, J. Pietraszko⁷,
 W. Przygoda², B. Ramstein¹⁴, L. Rehnisch⁷, A. Reshetin¹¹,
 A. Rustamov⁷, A. Sadovsky¹¹, P. Salabura², T. Scheib⁷, H. Schuldes⁷,
 J. Siebenson⁸, Yu.G. Sobolev¹⁵, S. Spataro^e, H. Ströbele⁷,
 J. Stroth^{7,3}, P. Strzempek², C. Sturm³, O. Svoboda¹⁵, A. Tarantola⁷,
 K. Teilab⁷, P. Tlusty¹⁵, M. Traxler³, H. Tsertos¹³, T. Vasiliev⁶,
 V. Wagner¹⁵, M. Weber⁹, C. Wendisch^{5,c}, J. Wüstenfeld⁵,
 S. Yurevich³, Y. Zanevsky⁶

[1]LIP-Laboratório de Instrumentação e Física Experimental de Partículas ,
 3004-516 Coimbra, Portugal

[2]Smoluchowski Institute of Physics, Jagiellonian University of Cracow, 30-059 Kraków,
 Poland

[3]GSI Helmholtzzentrum für Schwerionenforschung GmbH, 64291 Darmstadt, Germany

[4]Technische Universität Darmstadt, 64289 Darmstadt, Germany

[5]Institut für Strahlenphysik, Helmholtz-Zentrum Dresden-Rossendorf, 01314 Dresden,
 Germany

[6]Joint Institute of Nuclear Research, 141980 Dubna, Russia

[7]Institut für Kernphysik, Goethe-Universität, 60438 Frankfurt, Germany

[8]Excellence Cluster 'Origin and Structure of the Universe' , 85748 Garching, Germany

- [9]Physik Department E12, Technische Universität München, 85748 Garching, Germany
[10]II.Physikalisches Institut, Justus Liebig Universität Giessen, 35392 Giessen, Germany
[11]Institute for Nuclear Research, Russian Academy of Science, 117312 Moscow, Russia
[12]Institute of Theoretical and Experimental Physics, 117218 Moscow, Russia
[13]Department of Physics, University of Cyprus, 1678 Nicosia, Cyprus
[14]Institut de Physique Nucléaire (UMR 8608), CNRS/IN2P3 - Université Paris Sud, F-91406 Orsay Cedex, France
[15]Nuclear Physics Institute, Academy of Sciences of Czech Republic, 25068 Rez, Czech Republic
[16]LabCAF. Dpto. Física de Partículas, Univ. de Santiago de Compostela, 15706 Santiago de Compostela, Spain
[a]Also at ISEC Coimbra, Coimbra, Portugal
[b]Also at ExtreMe Matter Institute EMMI, 64291 Darmstadt, Germany
[c]Also at Technische Universität Dresden, 01062 Dresden, Germany
[d]Also at Frederick University, 1036 Nicosia, Cyprus
[e]Also at Dipartimento di Fisica Generale and INFN, Università di Torino, 10125 Torino, Italy

Abstract.

Hadron modifications in nuclear matter are discussed in connection to chiral symmetry restoration and/or hadronic many body effects. Experiments with photon, proton and heavy ion beams are used to probe properties of hadrons embedded in nuclear matter at different temperatures and densities. Most of the information has been gathered for the light vector mesons ρ , ω and ϕ . HADES is a second generation experiment operating at GSI with the main aim to study in-medium modifications by means of dielectron production at the SIS18/Bevelac energy range. Large acceptance and excellent particle identification capabilities allows also for measurements of strangeness production. These abilities combined with the variety of beams provided by the SIS18 allow for a characterization of properties of the dense baryonic matter properties created in heavy ion collisions at these energies. A review of recent experimental results obtained by HADES is presented, with main emphasis on hadron properties in nuclear matter.

1. Introduction

Sizable spectral modifications have been predicted by various theoretical models for hadrons embedded in cold or hot and dense nuclear matter. In this respect, most attention has been focused on properties of the light vector mesons (ρ , ω , and ϕ) as probes of chiral symmetry restoration (for reviews see [1, 2]). Early work based on QCD sum rules suggested a direct link between changes of the meson masses and QCD vacuum properties, characterized by a reduction of the expectation value of the two-quark condensate [3, 5]. More recent work shows however that, while such a link indeed exists, it is much more sophisticated than originally thought and offers a rather limited predictive power [1].

On the experimental side, a lot of experimental activities have been carried out over the last years investigating the light vector meson production off nuclei with proton and photon beams, and in heavy ion reactions. Two experimental approaches have been used to identify in-medium modifications of the vector mesons: (i) directly, via the reconstruction of their invariant mass distribution from the detected decay products and (ii) by quantifying the meson absorption in nuclei from the production yields and by connecting it to the in-medium width Γ_{tot}^* by model calculations (this method is used for $p(\gamma)+A$ collisions). The best suited final state are dileptons, which does not suffer strong final-state interactions (FSI) with the nuclear matter, but one has to cope with the small branching ratios ($\sim 10^{-5}$). The densities and temperatures reached in heavy ion collisions are of course higher, and larger effects can be expected but one has to properly

model the time evolution of the collision system to calculate dilepton radiation. Moreover, in order to access the true in-medium radiation one has to subtract the contribution of mesons decaying in the late state of the heavy ion collision, that is after the so called "freeze-out" where all interactions between the produced particles have ceased.

Results from $p(\gamma) - A$ experiments are somehow controversial: while the E325 experiment at KEK claims [4] the observation of a mass drop of the ρ meson in the e^+e^- invariant mass spectrum according to the Brown-Rho scaling [5], investigations at JLAB (CLAS) [6] does not corroborate such a conclusion showing only slight broadening of the ρ . Transparency measurements for the ω at ELSA/MAMI (CBELSA-TAPS) [8] and JLAB [7], and ϕ at COSY (ANKE) [9], LEPS at Spring8 [10] indicate large absorption of both mesons. However, the extraction of the in-medium widths from the measured nuclear transparency is not straightforward and even model dependant (for a review see T. Rodriguez's contribution to this conference).

In heavy-ion collisions, the search for vector meson spectral modifications via dilepton spectroscopy was pioneered by the CERES [11] and HELIOS [12] collaborations at the CERN SPS and the DLS experiment [13] at Bevalac. A low-mass pair excess, below the ρ/ω pole, above the yield expected from free hadron decays after the freeze-out, was reported and was widely discussed in many theoretical papers (for a review see [2]). Though the limited statistics of these experiments did not allow to derive firm conclusions, results obtained at SPS indicate that the excess is related to pions annihilating into the ρ meson, hence it is directly linked to the ρ in-medium spectral function. The breakthrough in this field was achieved with the high-statistics NA60 data set which allowed, for the first time, to extract the in-medium spectral function of the ρ meson [14]. Comparisons to various theoretical calculations show that the spectral function is mainly affected by two in-medium effects: (i) modification of the pion loop in the ρ meson self-energy and (ii) direct rho-meson couplings to low-mass baryon resonance-hole excitations [15]. Furthermore, it appears that the second mechanism plays the essential role in the observed melting of the ρ meson in hot and dense nuclear matter. On the other hand, the naive mass dropping scenario was found to be not supported by the data.

At top RHIC energies, the situation is less clear: first results from most central $Au + Au$ collisions at $\sqrt{s}=200$ GeV obtained by PHENIX indicated even larger excess than at SPS [16]. However, new measurements performed by STAR (see contributions to this conference) do not corroborate this observation.

On the other side of the energy scale at 1-2 AGeV, results of the DLS experiment could not find a satisfactory explanation for a long time. Dielectron spectra measured even in light $C + C$ collisions were not described by any model calculation showing a large excess in the mass $0.6 > M_{e^+e^-} > 0.15$ GeV/ c^2 range. However, nuclear matter probed in this energy range is dominated by baryons (nucleons and up to 30% low mass-baryonic resonances) and it has a different composition from the meson (mainly pion) dominated one probed at SPS. Therefore, it was not clear if the excess is due to some particular features of baryonic sources not properly modeled in the calculations or true in-medium effects.

A clarification of this dilemma was one of the main reasons to build the HADES experiment at GSI [17]. It is a second generation versatile detector, shown in Fig.1, with excellent particle identification capabilities and large acceptance. HADES (High Acceptance DiElectron Spectrometer) has, for the first time in this energy regime, the capability to simultaneously measure various rare probes like dielectrons, single (kaons, hyperons) and double strange hadrons (Ξ^- (1321) and ϕ mesons). The ability to study strangeness production is particularly interesting from the point of view of still unsettled questions of kaon in-medium properties (for a review see [18]). Experiments performed at GSI by means of KAOS and FOPI detectors provided many interesting data. However, further precise measurements of kaon flow, low transverse momentum distributions of kaons and ϕ production are necessary to fully characterize kaon production in

heavy ion collisions. Furthermore, double strange hyperons have never been measured before at SIS18 energies and likewise first data on ϕ meson production have been only recently provided by HADES and FOPI detectors.

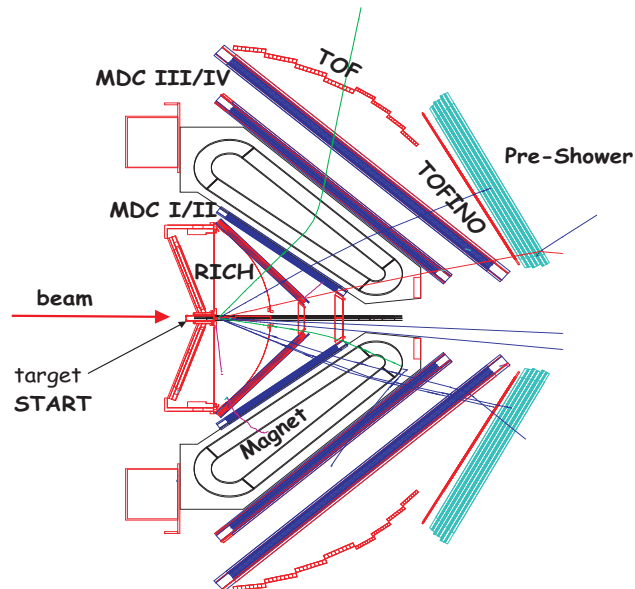


Figure 1. Schematic layout of the HADES detector. A RICH detector with gaseous radiator, carbon fiber mirror and UV photon detector with solid CsI photocathode is used for electron identification. Two sets of Mini-Drift Chambers (MDCs) with 4 modules per sector are placed in front and behind the toroidal magnetic field to measure particle momenta. A time of flight wall TOF/TOFINO (the latter one replaced in 2010 by a high granularity RPC) accompanied by a Pre-Shower detector at forward angles is used for additional electron identification and trigger purposes. The target is placed at half radius off the center of the mirror. For reaction time measurement, a START detector is located in front of the target [17]

Using the variety of proton, deuteron and ion beams HADES can study elementary and heavy ion reactions creating dense (up to $3\rho_0$) and hot (with temperatures up to $T=80$ MeV) nuclear matter with relatively long life time (~ 10 fm/c). With its future scientific programme at SIS100 at FAIR it will also cover the 8 – 10 AGeV energy range, where there is no dielectron data up to now. Therefore it also will, together with the future Compressed Baryonic Matter experiment of FAIR [19], provide further valuable data to complete our understanding of the nuclear matter phase diagram in the baryon rich region.

2. Experimental programme of HADES

The HADES programme realized so far can be divided into three strongly interconnected parts. Experiments studying dielectron, pion and baryon resonance production in proton-proton (at 1.25, 2.2 and 3.5 GeV) and $d + p$ (at 1.25 GeV) reactions provided important constraints on contributions of various e^+e^- sources and allowed to establish model independent reference spectra for studies of proton-nucleus and nucleus-nucleus collisions. $p + p$ collisions at 3.5 GeV provided also valuable new data on hyperon $\Sigma(1385)$ and $\Lambda(1405)$ production. The vector mesons and the neutral kaon productions were investigated in $p + Nb$ collisions at 3.5 GeV to search for meson modifications in cold nuclear matter. Small $C + C$ and medium size $Ar + KCl$ collision

systems were explored in the 1–2 AGeV energy range to verify the origin of the dielectron excess observed in DLS experiments and to study strangeness production (ϕ , $K^{-,+0}$, Λ , $\Xi^{-}(1321)$). Studies of nucleus-nucleus collision systems has been continued in 2012 with $Au + Au$ collisions at 1.25 GeV. Below we present highlights of the results obtained so far, with emphasis on hadron in-medium properties.

3. Results from N-N collisions

The special character of e^+e^- production in $N - N$ collisions in the 1-2 GeV beam energy range is given by a strong contribution of baryonic sources: Dalitz decays of nucleon resonances $R \rightarrow Ne^+e^-$ (mainly $\Delta(1232)$) and $N - N$ bremsstrahlung, and a strongly rising excitation functions of the η meson production [20]. The baryonic sources completely determine the e^+e^- invariant mass distribution above the π^0 mass at beam energies below the η meson production threshold ($E_{beam}^{thr}=1.25$ GeV) [21]. The latter contributes via $\eta \rightarrow e^+e^-\gamma$ decay at the same level as the baryonic sources already around 1.6 GeV. The vector meson production is small because of the high production threshold ($E_{beam}^{thr}=1.88$ GeV for ω) and adds an important contribution to the invariant mass spectrum at $M_{e^+e^-} > 0.6$ GeV/ c^2 . While the exclusive ω and η production in $p + p$ reactions close to the production threshold is very well known, the data on ρ are scarce. Furthermore, in contrast to the ω and ϕ production mechanisms, which essentially do not show resonance contributions, a strong coupling of the ρ meson to the low-mass baryonic resonances ($D_{13}(1520), P_{13}(1720), \dots$) has been predicted by many models (see for example [22, 23]). Since the ρ meson is a broad resonance these couplings can lead to the spectral function very different from a simple Breit-Wigner distribution even in elementary reactions. One should underline that a detailed understanding of these couplings is a prerequisite for any conclusions on in-medium modifications in nuclear matter. This statement holds also for the situation at higher beam energies where, as already discussed above, baryonic effects are of major importance for the interpretation of NA60 and CERES data. One should also stress that decays processes like $R \rightarrow Ne^+e^-$ (Dalitz) and $R \rightarrow \rho(\rightarrow e^+e^-)N$ are strongly linked and should not be in general treated as a two separate decay channels. A natural connection should be provided by a structure of the electromagnetic transition form factors in the time-like region, i.e its dependence on the virtual photon (or e^+e^- invariant) mass. Calculations performed within the extended Vector Meson Dominance (VMD) model [26] and the two component model [27, 28] indeed show the importance of the vector mesons in such transitions. However, new precise data from proton and, in particular, pion induced reactions on such decays are needed to provide more constraints for calculations. We come to this issue in discussion of the HADES data obtained at higher beam energy of 3.5 GeV.

The other silent feature of dielectron production in $N + N$ reactions is a very strong isospin dependence. This feature was already demonstrated by the DLS experiment measuring excitation functions of the pair production in $p + p$ and $d + p$ collisions in the beam energy range E_{beam} 1-4.88 GeV [25]. Though the statistics gathered in these experiments is limited and the systematic errors related to normalization are large, one can clearly see that there is a strong increase of the non-trivial pair yield (in the $M_{e^+e^-} > M_{\pi^0}$ range) in $d + p$ reactions over the one measured in $p + p$ below 2 GeV, with maximum around $E_{beam}=1.25$ GeV. New data obtained by HADES stimulated significant progress in understanding this phenomenon. Fig. 2 shows the e^+e^- invariant mass distributions obtained in $p + p$ and, for the first time, in quasi-free $n + p$ reactions, the latter one selected by tagging the proton spectator from $d + p$ collisions, at $E_{beam}=1.25$ GeV. While the $p+p$ data can be described rather well by the incoherent superposition of the π^0 and $\Delta(1232)$ Dalitz decays, the $p + n$ data shows a large excess over these two contributions at $M_{e^+e^-} > M_{\pi^0}$. The situation is not changed by adding a small η contribution in the $p + n$ case, appearing because of the neutron momentum distribution

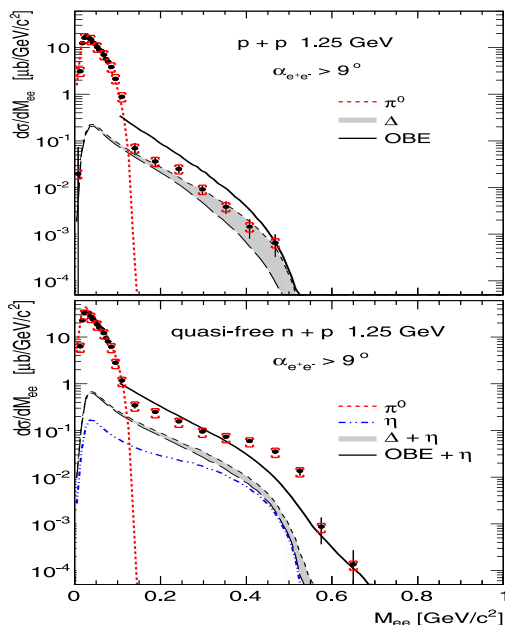


Figure 2. Electron pair differential cross sections as a function of invariant mass (full circles) measured in $p+p$ reactions (upper panel) and in quasi-free $n+p$ reactions (lower panel) at 1.25 GeV. Systematic errors (constant in the whole mass range) are indicated by (red) horizontal bars, statistical errors by vertical bars. Expected contributions from π^0 , $\Delta(1232)$ and η Dalitz decays obtained by PLUTO event generator are shown separately [21]. Solid curves show predictions from the One Boson Exchange Model [29]

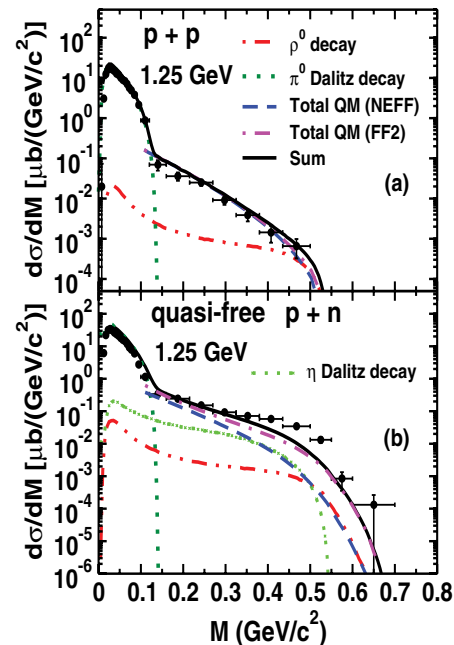


Figure 3. Experimental data (same as on in Fig. 1) compared to the One Boson model [30]. Results without (NEFF) and with (FF2) incorporation of the electromagnetic form factor of charged pions are shown separately. Solid curves show sum of these contributions with the subthreshold ρ production

inside deuteron. The latter one is very well constrained by the known η meson production cross section and nucleon momentum distribution inside the deuteron (see for details [21]). The shaded area shows the uncertainty related to the electromagnetic transition form-factor of the $\Delta(1232) \rightarrow Ne^+e^-$ decay calculated here within the two-component (quark core and pion cloud) model [28]. The solid curve shows predictions of [29] based on One-Boson Exchange model of the bremsstrahlung process taking into account the coherent sum of resonant ($\Delta(1232)$) and non-resonant (so called "quasi-elastic" bremsstrahlung) contributions [29]. In Fig. 3, we show results of recent OBE calculations [30] compared to HADES data which provide a better description. In particular, the very different shape of the $p+n$ data is better accounted for, due to the incorporation of the electromagnetic form factor of the charged pion. This contribution is possible since, in contrast to the $p+p$ reaction a charged pion can be exchanged. Although, the theoretical description of the $p+n$ data is not yet finally settled, the data allow to construct the experimentally derived $N+N$ reference spectrum, which we use for heavy ion reactions to account for the contribution of the baryonic sources.

4. Results from p-A collisions

$p + p$ and $p + Nb$ collisions at a beam energy of 3.5 GeV have been studied by HADES with the main goal to search for in-medium modification of vector mesons in cold nuclear matter. The large acceptance of the detector and the low energy of the beam allow for a detection of e^+e^- pairs down to low momenta ($p_{e^+e^-} < 1.0$ GeV/c) which are not in the CLAS and E325 experiments. Differential e^+e^- production cross sections as a function of the e^+e^- invariant mass (shown in Fig. 4), the momentum and the rapidity have been measured for both reactions [31]. The direct comparison of the measured distributions to the yields expected from the known hadronic sources (from a PYTHIA calculation) is shown for $p + p$ collisions in Fig. 4 [24]. It reveals an unexplained strength below the vector meson pole which becomes even more pronounced in proton-nucleus collisions. As already discussed in the previous sections, one can expect such additional strength by a strong coupling of the ρ meson to low-mass baryonic resonances, which are not included in PYTHIA. They should be reflected in the respective electromagnetic transition form factors of $R \rightarrow Ne^+e^-$ decays. Indeed, calculations [22] including the form factors of $\Delta \rightarrow Ne^+e^-$, obtained from the two component model [28], describe the missing yield but leave no space for a contribution from higher-mass resonances. Since the latter one are poorly known, an alternative approach, based on a resonance model, is commonly used in transport models to describe these contributions. Namely, the dilepton decays of resonances with known decay branches to $N\rho$ are modeled as two step process $R \rightarrow \rho N \rightarrow Ne^+e^-$ using a e^+e^- mass dependent decay width calculated within the VMD model. Indeed, such approach can describe our data, as shown by calculations performed with GiBUU [22], assuming strong contributions from $D_{13}(1520)$, $S_{31}(1620)$, $P_{13}(1720)$ and $F_{35}(1905)$. However, as the authors of [22] conclude, this result should be taken with caution since the exact production cross sections of the resonances and their decay branches into ρN are subject of large uncertainties. We hope that further studies of exclusive reaction channels $p + p \rightarrow \pi NN$ and $p + p \rightarrow ppe^+e^-$, reconstructed in HADES, will shed more light on this important aspect.

Coming back to the $p + Nb$ data, we show in Fig. 5 comparison of the e^+e^- invariant mass distribution to the one measured in $p + p$ reactions for two momentum bins of the outgoing dielectron pair. Here, the $p + p$ cross sections have been scaled up by a ratio of the total cross sections for both reactions and the averaged numbers of participants calculated with a Glauber model: $\sigma_{pNb}/\sigma_{pp} \times \langle A_{part}^{pNb} \rangle / \langle A_{part}^{pp} \rangle$. With such scaling π^0 production measured in $N + N$ describe describe our $C + C$ data (see next section), and also, (see Fig. 5), pion Dalitz yield in $p + Nb$. On the other hand, a strong increase of the e^+e^- yield below the vector meson pole above the $p + p$ reference is visible for low momenta $p_{e^+e^-} < 0.8$ GeV/c (see Fig.6, left panel).

In order to better quantify this excess we subtract first, the ω peak in both data samples and further subtract the scaled $p + p$ dielectron yield from the $p + Nb$ yield. The difference, shown in Fig. 6-right panel, represents the additional e^+e^- radiation excess due to the medium. For the scaled spectra the resulting excess for $p_{e^+e^-} < 0.8$ GeV/c corresponds to a factor 1.5 ± 0.3 of the $p + p$ data in the invariant mass region between 0.3 and 0.7 GeV/c² and shows an exponential decrease with an additional enhancement directly below the vector meson pole mass, i.e. between 0.6-0.7. Note that this enhancement is exactly at the position where a discrepancy is observed when comparing the $p + p$ data with the PYTHIA calculation (Fig. 4), indicating that both observations might be linked by the same physical process. This might be interpreted as a fingerprint of the contribution of secondary processes of the type $p + p \rightarrow \pi X$, $\pi N \rightarrow R \rightarrow Ne^+e^-$ adding also to this mass region because of the aforementioned strong resonance- ρ couplings. On the other hand, most of model calculations based on hadronic many-body interactions predict that such couplings strongly modify the in-medium ρ meson spectral function. Therefore, final conclusions about in medium modifications of the ρ meson in cold

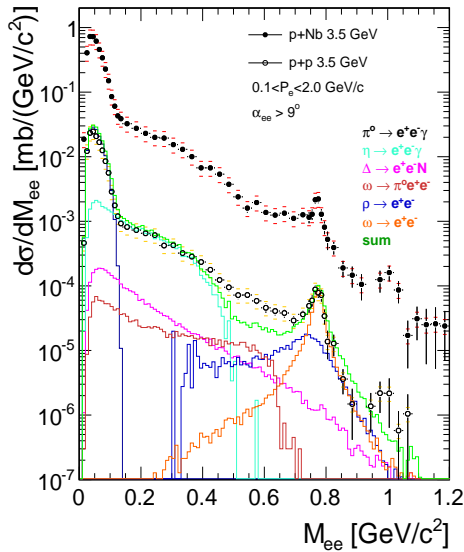


Figure 4. Comparison of dielectron cross sections as a function of the invariant mass measured in $p + p$ and $p + Nb$ collisions at beam energy of 3.5 GeV. For the $p + p$ data, a PYTHIA dilepton cocktail composed of various e^+e^- sources, defined in the legend, is displayed in addition [31]

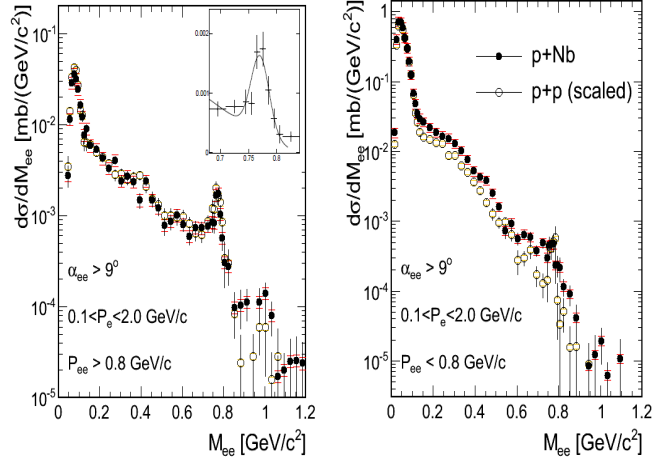


Figure 5. Comparison of the invariant mass spectra for e^+e^- pairs with $P_{e^+e^-} > 0.8$ GeV/c (left panel) from $p + p$ and $p + Nb$. The inset shows a linear zoom into the vector meson region together with a fit to the ω peak for the $p + Nb$ data. Right: for pairs with $P_{e^+e^-} < 0.8$ GeV/c. The $p + p$ data have been scaled as described in the text [31]

nuclear matter can be derived only, if a consistent treatment of the spectral shape of the meson in the medium together with a correct handling of the additional yield from secondary reactions is achieved.

As the ω meson is concerned, we observe that for slow pairs the yield at the ω pole is not reduced, however, the underlying smooth distribution is enhanced. Thus, the yield in the peak is almost zero within errors. This indicates a strong ω absorption in contrast to the pairs from the underlying continuum. Assuming that the ω cross section scales with the mass number as $\sigma_{pNb} = \sigma_{pp} \times A^\alpha$ we obtain $\alpha = 0.38 \pm 0.29$ for slow pairs and $\alpha = 0.67 \pm 0.11$ for $p_{e^+e^-} > 0.8$ GeV/c. Furthermore, an analysis of the ω width shows, within the error bars, no significant broadening. Both observations are in line with the results of the CBELSA-TAPS experiment [32], although one should note that in contrast to the $p + A$ reactions for the photon induced reactions no initial state effects and consequently a stronger scaling could be expected.

5. Results from A-A collisions

In the 1 – 2 AGeV energy range, particle production in heavy-ion collisions is dominated by pion production which originates mainly from the $\Delta(1232)$ resonance. Multiplicities of heavier mesons, mainly η , are already very low (of order 1 – 2%). Production multiplicities for π^0 and η mesons are known from their decay into real photons from former TAPS measurements at GSI [33]. The dielectron invariant-mass distributions measured with HADES in the light $C + C$ (at 1.0, AGeV) [34] and the medium-heavy $Ar + KCl$ (at 1.756 AGeV) [35] systems are shown in Fig. 7.

The spectra are normalized to the mean of the charged pion (π^+ , π^-) yields, measured

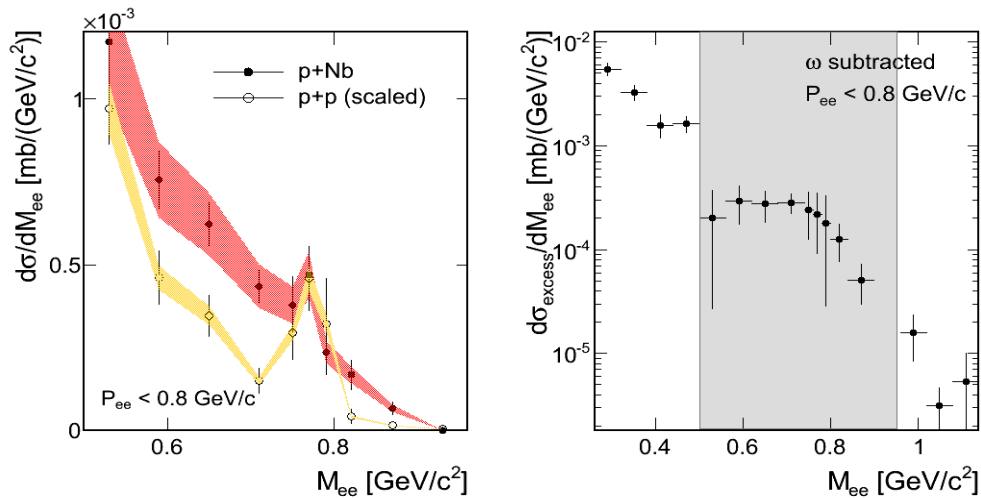


Figure 6. Same as in Fig. 5 but zoomed into the vector meson region. The shaded bands represent the systematic uncertainties due to the normalization. Right: Excess yield in the $p+Nb$ data after subtraction of the scaled $p+p$ reference data (the ω contribution has been subtracted in both data samples). The grey region corresponds to the invariant mass range plotted in the left picture [31]

independently by HADES, and extrapolated to the full solid angle. At this energy and for these collision systems, it is a good measure of neutral pion multiplicity. The differential distributions obtained in such a way are compared to the expected mesonic e^+e^- cocktail from the π^0, η Dalitz and ω decays according to the measured (for π^0 and η) and extrapolated (from the m_T scaling for ω) multiplicities. One should underline that the ω peak visible in the invariant mass distribution in $Ar+KCl$ collisions allows for the first measurement of meson production at such a low energy (below its free $N-N$ threshold). As one can see, the e^+e^- cocktail composed from the meson decays does not explain the measured yields for both collision systems and leave room for a contribution expected from the baryonic sources discussed above: resonance Dalitz decays (mainly $\Delta(1232)$) and nucleon-nucleon bremsstrahlung. This conclusion is also supported by our analysis of the shape of excitation function of the missing contribution that appears to be very similar to the one measured for pions, governed by $\Delta(1232)$ creation, but very different from the one established for the η meson [35].

In order to search for a true in-medium radiation off the dense nuclear phase of collisions we compare e^+e^- production rates found in nucleus-nucleus reactions with a proper superposition of the production rates measured in elementary collisions. For this purpose, we plot in Fig. 8 the ratio of the pair multiplicities measured in nucleus-nucleus collisions, shown in Fig. 7 (and also for $C+C$ at 2 AGeV), to the averaged $1/2(M_{pp}^{e^+e^-} + M_{pn}^{e^+e^-})/M_{\pi^0}$ obtained from the e^+e^- cross sections shown in Fig. 2 and the known π^0 cross section for the elementary reactions. Furthermore, before the ratios are computed we subtract for all distributions the respective η Dalitz contributions. The latter is motivated by a very different excitation function of the η meson production in nucleus-nucleus and nucleon-nucleon reactions and hence allows for comparison of collision systems measured at different beam energies. Normalization to the M_{π^0} takes into account the beam energy dependence of baryonic sources discussed above and also the dependence of particle production on system-size via scaling with an average number

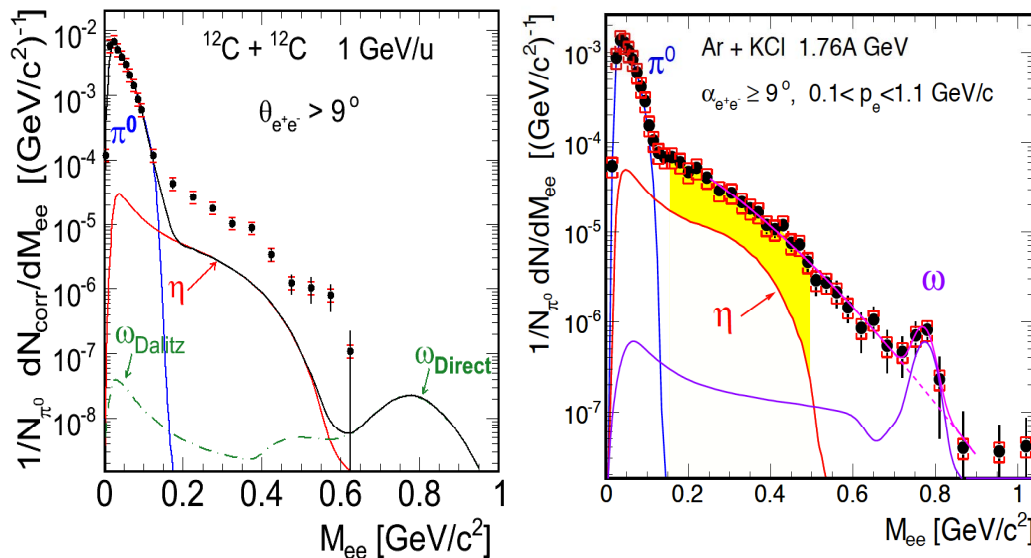


Figure 7. Left: e^+e^- production rates normalized to the π^0 yield as a function of the invariant-mass distribution measured in $C + C$ collisions at 1 AGeV compared to thermal dielectron cocktail of mesonic sources (π^0, η, ω) after freeze-out [34]. Right: Similar distributions but obtained for $Ar + KCl$ collisions at 1.756 AGeV [35]. Shaded area shows invariant mass region where the pair excess from in-medium radiation has been identified (for details see text). Different widths of the ω peak in simulated cocktails accounts for different mass resolution in both experiments

of participants A_{part} , which holds at SIS18 energy range (for more details see [35]). As one can see all distributions agree in the π^0 mass range confirming our normalization procedure. Furthermore, the ratio is consistent, within statistical and systematic errors, with the one for $C + C$ collisions at 1 and 2 AGeV. It means that indeed, pair production in the mass range $M_{e^+e^-} < 0.6 \text{ GeV}/c^2$ in $C + C$ collisions can be described as sum of contributions stemming from (i) baryonic sources, extracted from the $N + N$ collisions, which yield scale as pion production and (ii) the η, π^0 mesons accounting for the radiation after freeze-out. This observation explains the long standing "DLS puzzle" of the unexplained yield measured in $C + C$ collisions by not correctly accounted baryonic contributions. In this context we emphasize that the DLS and HADES data agree within errors bars as shown by a dedicated analysis [34].

However, a significant excess (2.5-3) with respect to the $N + N$ reference is visible for the $Ar + KCl$ system above the π^0 mass, signaling an additional contribution from the dense phase of the heavy ion collision. This means that going to the larger collision system $Ar + KCl$ (A_{part} for $Ar + KCl \simeq 40$ should be compared to $A_{part} \simeq 8$ for $C + C$ for our trigger conditions) a stronger than linear scaling of the pair production with A_{part} is observed. This observation can be interpreted as a signature of the onset of a contribution of multi-body and multi-step processes in the hot and dense phase created in collisions of nuclei of sufficiently large size. In this context, the propagation of short-lived baryonic resonances seems to play a main role. The penetrating nature of the dilepton probe allows to observe an effect of "shining" of the baryonic matter integrated over the whole collision time. A further important test of this scenario will be provided by data recently obtained from $Au + Au$ collisions at 1.25 GeV.

Interesting new results on the vector meson production in heavy-ion collisions at SIS18 have also been obtained from analysis of $Ar + KCl$ data. Besides the ω signal discussed above, a surprisingly strong ϕ meson production have been found from an analysis of the K^+K^- final

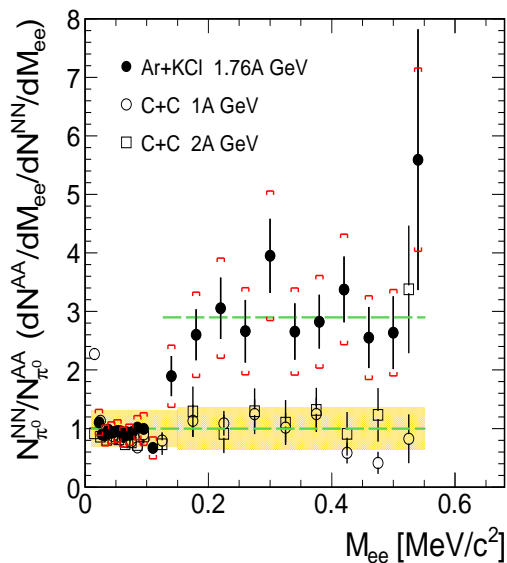


Figure 8. Ratio of e^+e^- invariant mass distributions measured in Ar+KCl and C+C with subtracted η meson contribution to the $N + N$ reference spectrum, obtained as described in text. Total errors, statistical and systematic are added quadratically and indicated by the shaded band [35].

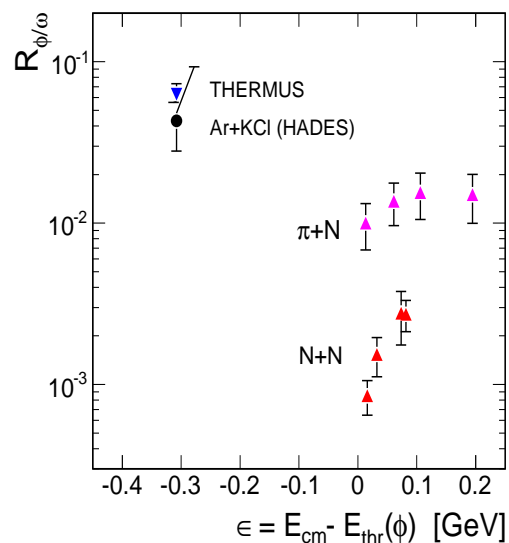


Figure 9. Comparison of the measured $R_{\phi/\omega}$ ratio (HADES) and statistical model value (THERMUS fit) as well as a compilation of data from the $p+p$ and $\pi+N$ reactions (see text). The ratio is plotted as a function of the excess energy above the threshold for the exclusive production in $p+p$ and $\pi+N$ reactions [35].

state (see Fig. 10) [36]. The acceptance corrected ϕ/K^- ratio is found to be 0.37 ± 0.13 which translates into a fraction of $18 \pm 7\%$ of negative kaons coming from ϕ decay. Furthermore, assuming that non-resonant K^+K^- production is of the same size, as it is known from $N+N$ reactions, an even larger contribution of reactions other than strangeness exchange (π^- hyperon $\rightarrow K^-N$), assumed before to be the dominant process in K^- production, should be expected. This, for example, can indicate that the ϕ meson is produced in multi-step processes involving short-lived resonances. Such scenario is corroborated by BUU transport calculations [37] which reproduce the yields and spectral distributions of K^+K^- and ϕ mesons.

Fig. 9 shows the ratio of the ϕ to ω multiplicities measured in $Ar + KCl$ collisions at 1.756 AGeV, together with predictions of the statistical model THERMUS and results from elementary reactions [35, 36]. The data points are plotted as a function of the excess energy above the production threshold for the exclusive ϕ production in $p+p$ and $\pi+N$ reactions, respectively. One can see from this comparison that in the heavy-ion reaction $R_{\phi/\omega}$ is more than one order of magnitude larger than in $N+N$ collisions and also at least a factor 3–5 larger than in pion-induced processes. On the other hand, the ratio is consistent with the thermal model assuming full thermalization and no suppression due to OZI rules. The ratio could of course also be influenced by different absorption processes of both mesons in nuclear matter. Indeed, the results from cold matter experiments, mentioned in the introduction, indicate larger absorption of the ω meson as compared to the ϕ what could enhance the in-medium $R_{\phi/\omega}$. The effect of ω absorption and the absence of such effect on the ϕ was also observed by NA60 in $In + In$ collisions at 158 AGeV [38, 39].

In-medium effects on kaons have been studied by means of K_s^0 meson transverse momentum distributions in Ar+KCl collisions at 1.76 AGeV taking advantage of the good acceptance of

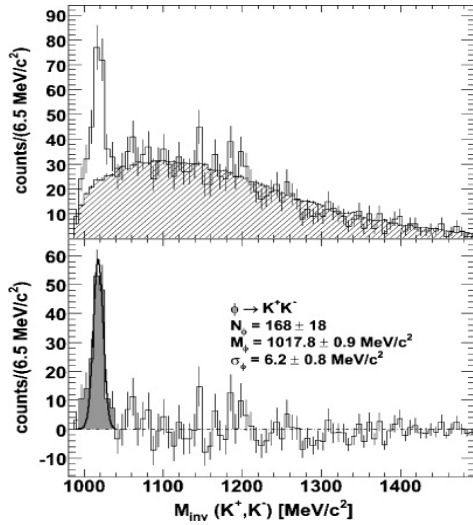


Figure 10. Invariant mass distribution of K^+K^- pairs (top). The combinatorial background (shaded area) is obtained by the mixed-event technique. The background-subtracted distribution (bottom) shows a ϕ meson signal (grey area with a Gaussian fit) [36]

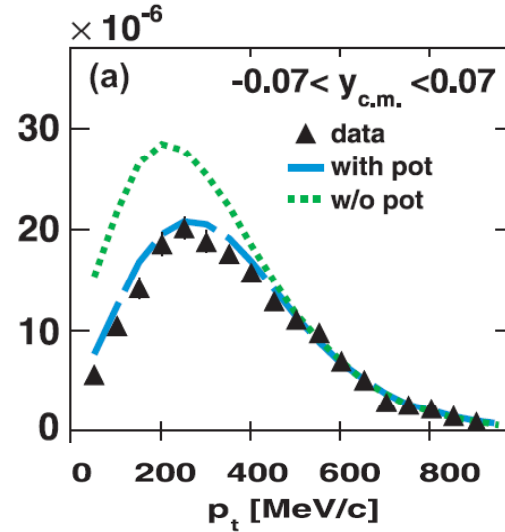


Figure 11. p_t distribution of the experimental K_S^0 data (full triangles) together with the results of the IQMD model including a repulsive K^0 -nucleus potential of 46 MeV (dashed curves) and without potential (dotted curves) [40].

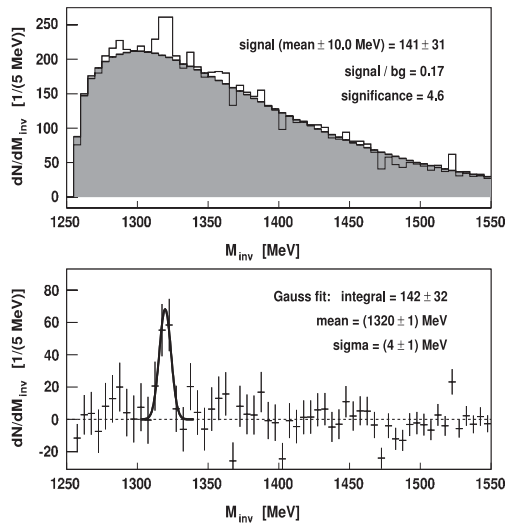


Figure 12. Top: $\Lambda - \pi^-$ invariant mass distribution with background (hatched histogram) calculated with event mixing. Bottom: The invariant-mass distribution after background subtraction. The full curve represents a Gaussian fit to the $\Xi^-(1321)$ signal [42]

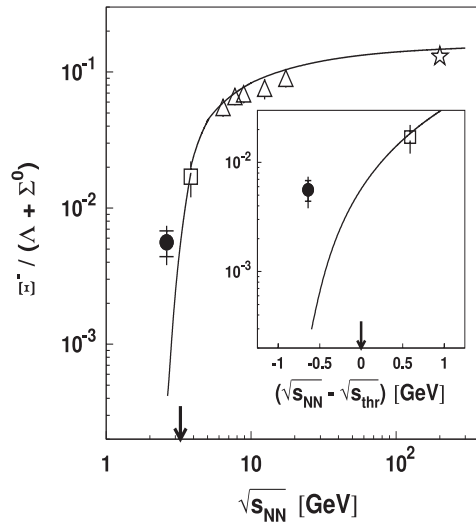


Figure 13. The excitation function of the $\Xi^-(1321)$ to $\Lambda + \Sigma^0$ ratio measured by HADES (full circles) and other high energy experiments (empty symbols) compared to statistical model predictions [42] (solid curves). The arrow depicts the $\Xi^-(1321)$ threshold [42]

HADES at low transverse momentum for the $K_S^0 \rightarrow \pi^+\pi^-$ reconstruction [40]. We compared p_t distributions for different rapidity bins with the corresponding results by the IQMD transport

approach with and without taking into account a repulsive K^0 -nucleus potential. For all rapidity bins, but most evidently at mid-rapidity (shown in Fig. 11), data support calculations with the repulsive potential. Our data suggest a repulsive in-medium K^0 potential of about 40 MeV strength which is slightly higher as compared to results obtained from experiments studying K_s^0 production off nuclei [41].

The ability of HADES for the selection of displaced secondary vertices arising from weak decays and the high statistics accumulated for the collision system $Ar + KCl$ at 1.76 A GeV allowed to investigate the deep-threshold production ($\sqrt{s_{NN}} - \sqrt{s_{thr}} = 640$ MeV) of the double-strange $\Xi^-(1321)$ hyperon [42]. The $\Xi^-(1321)$ was reconstructed in the $\Lambda - \pi^-$ invariant mass distribution, shown in Fig. 12, thanks to a high-purity signal of Λ identified in the $p - \pi^-$ invariant mass distribution. Fig. 13 shows the ratio of production rates of $\Xi^-(1321)$ and $\Lambda + \Sigma^0$ as a function of the total CM energy in $N + N$ collisions measured by HADES and other high-energy experiments. The reconstructed strength of the signal is compared to calculations performed for $Au + Au$ collisions with the statistical model of [43]. While high-energy data are well described, the present experimental ratio is underestimated, by the model, by a factor of 10 yielding 4×10^{-4} . Utilizing the statistical model package THERMUS [44] and fitting all particle yields, except $\Xi^-(1321)$, measured in $Ar + KCl$ collisions we obtained temperature $T = 73 \pm 5$ MeV and a chemical potential $\mu_b = 780 \pm$ MeV [45] and an even lower (by factor 2) as compared to [43] ratio of $\Xi^-(1321)/\Lambda + \Sigma^0$ production. In the recent work [46], the strong $\Xi^-(1321)$ production observed in our experiment has been accounted for by strange exchange reactions of the type hyperon-hyperon $\rightarrow N\Xi^-(1321)$. nevertheless, further high statistics measurements, in particular of the differential production cross sections, are needed to shed more light on this problem.

6. Conclusions

We have presented new results on dielectron and strangeness production in $N - N$, proton-nucleus and nucleus-nucleus collisions. The e^+e^- invariant mass distributions measured in $p + p$ and $p + n$ collisions at 1.25 GeV reactions provide an important reference for heavy ion collisions. In particular, we find that the anomalous increase of the pair production in $p + n$ collisions, stemming presumably from the bremsstrahlung process, is the main contribution explaining dielectron production in the light $C + C$ collisions. However, we also observe a significant pair excess in the $0.15 < M_{e^+e^-} < 0.5$ GeV/ c^2 mass range with respect to this $N + N$ reference for the medium size $Ar + KCl$ system, signaling an additional contribution from the dense phase of the heavy ion collisions. We interpret this as a result of continuous radiation ("shining") from short lived baryonic resonances (mainly $\Delta(1232)$) regenerated in multi-step processes in dense nuclear matter. An important verification of this scenario will be provided by $Au + Au$ data recently collected by HADES.

We find that ρ meson production in our energy range is strongly affected by a strong coupling to low-mass baryonic resonances which is reflected in a significant broadening of the meson spectral function already visible in $p + p$ reactions. These interactions might lead to a further meson modification in cold and dense nuclear matter but a quantitative assessment can only be made after these couplings are better constrained. Presented results from $p + p$, $p + Nb$ collisions at 3.5 GeV and further planned studies of the resonance Dalitz decays in exclusive reaction channels are of utmost importance.

Studies of the ω production off nucleus show a strong absorption of the meson in nuclear matter in accordance with the results from photon induced reactions. The ω and ϕ signals have also been reconstructed in $Ar + KCl$ collisions at energies below the $N - N$ production threshold. A surprisingly large $R_{\phi/\omega}$ production ratio (more than one order of magnitude larger than in $N + N$ collisions) has been found, indicating no suppression for the ϕ production and

consequently a significant contribution to the K^- production. Also a strong enhancement of the double strange $\Xi^-(1321)$ production has been found, even above predictions (factor 10) of statistical models. This intriguing results calls for further experimental studies which will be performed with larger collisions systems.

Our programme of investigations of the in medium kaon potential has been started with the measurement of K^0 production in $Ar + KCl$ revealing a strong ($U=40$ MeV) repulsive potential. Further studies of K_0 potential in cold nuclear matter are on the way with already collected $p + Nb$ data. Charged kaon production by means of flow measurements are planned with future $Ag + Ag$ collisions.

The author thanks GSI Darmstadt for support for this work. The collaboration gratefully acknowledges the support by CNRS/IN2P3 and IPN Orsay (France), LIP Coimbra, Coimbra (Portugal): PTDC/FIS/113339/2009, SIP JU Cracow, Cracow (Poland): N N202 286038 28-NN202198639, Helmholtz-Zentrum Dresden-Rossendorf (HZDR), Dresden (Germany): BMBF 06DR9059D, TU München, Garching (Germany) MLLMünchenDFGEClust: 153VHNG- 330, BMBF 06MT9156 TP5 TP6, GSI TMKrue 1012, NPI AS CR, GSI TMFABI 1012, Rez, Rez (Czech Republic): MSMT LC07050 GAASCRIAA100480803, USC - S. de Compostela, Santiago de Compostela (Spain): CPAN:CSD2007- 00042, Helmholtzalliance HA216/EMMI.

References

- [1] S. Leupold, V. Metag and U. Mosel, Int. J. Mod. Phys. E **19**, 147 (2010).
- [2] R. Rapp and J. Wambach, Adv. Nucl. Phys. **25**, 1 (2000).
- [3] T. Hatsuda and S. H. Lee, Phys. Rev. C **46** 34 (1992).
- [4] M. Naruki et al., Phys. Rev. Lett. **96** 092301 (2006).
- [5] G. E. Brown and M. Rho, Phys. Rev. Lett. **66** 2720 (1991).
- [6] R. Nasseripour et al. (CLAS Collaboration), Phys. Rev. Lett. **99** 262302 (2007).
- [7] M. H. Wood et al. (CLAS Collaboration), Phys. Rev. Lett. **105** 112301 (2010).
- [8] M. Kotulla et al. (CBELSA/TAPS Collaboration), Phys. Rev. Lett. **100** 192302 (2008).
- [9] A. Polyanskiy et al. (ANKE Collaboration) Phys. Lett. B **695** 74 (2011).
- [10] T. Ishikawa et al., Phys. Lett. B **608** 215 (2005).
- [11] G. Agakishiev et al. (CERES Collaboration), Phys. Rev. Lett. **75** 1272 (1995).
- [12] M. Masera (HELIOS Collaboration), Nucl. Phys. A **590** 93C (1995).
- [13] R. J. Porter et al. (DLS Collaboration), Phys. Rev. Lett. **79** 1229 (1997).
- [14] R. Arnaldi et al. (NA60 Collaboration), Phys. Rev. Lett. **96** 162302 (2006).
- [15] H. van Hees and R. Rapp, Nucl. Phys. A **806** 339 (2008).
- [16] S. Afanasiev et al. (Phenix collaboration), Phys. Rev. C **81** 034911 (2010).
- [17] G. Agakishiev et al. (HADES Collaboration), Eur. Phys.J.A **41**, 243 (2009).
- [18] C. Fuchs Prog. Part. and Nucl. Phys., **56**, 1 (2006).
- [19] C. Höhne et al. (CBM) collaboration, contribution to this conference
- [20] G. Agakishiev et al. (HADES Collaboration), Phys. Rev. C **85**, 054005 (2012).
- [21] G. Agakishiev et al. (HADES Collaboration), Phys. Lett. B **690**, 118 (2010).
- [22] J. Weil, H. van Hees and U. Mosel, arXiv:1203.3557, O. Buss et al., Phys.Rept. **512** 1 (2012).
- [23] K. Schmidt et al., Phys. Rev. C **79**, 064908 (2009).
- [24] G. Agakishiev et al. (HADES Collaboration), Eur. Phys. J. A **48**, 64 (2012).
- [25] W.K Wilson et al. (DLS Collaboration), Phys. Rev. C **57**, 1865 (1998).
- [26] M. I. Krivoruchenko et al., Ann. Phys. **296**, 299 (2002).
- [27] G. Ramalho, M.T. Pena, Phys.Rev. D. **85**, 113014 (2012).
- [28] Q. Wan, F. Iachello, Int. J. Mod. Phys. A **20**, 1846 (2005) 1846.
- [29] L. P. Kaptari and B. Kämpfer, Nucl. Phys. A **764**, 338 (2006); Phys. Rev. C **80**, 064003 (2009).
- [30] R. Shyam and U. Mosel Phys. Rev. C **82**, 062201 (2010).
- [31] G. Agakishiev et al., (HADES Collaboration), Phys. Lett.B **715**,304 (2012).
- [32] M. Nanova et al. (CBELSA-TAPS Collaboration), Phys. Rev. C **82**, 035209 (2010).
- [33] R. Averbeck et al., (TAPS Collaboration), Z. Phys. A **359**, 65 (1997).
- [34] G. Agakichiev et al., (HADES Collaboration), Phys. Lett. **663**, 43 (2008).
- [35] G. Agakichiev, et al., (HADES Collaboration), Phys. Rev.C **84**, 014902 (2011).

- [36] G. Agakishiev et al. (HADES Collaboration), *Phys. Rev. C* **80**, 025209 (2009).
- [37] H. Schade, Gy. Wolf, B. Kämpfer, *Phys. Rev. C* **81**, 034902 (2010).
- [38] R. Arnaldi et al. (NA60 Collaboration), *Eur. Phys. J. C* **61** 711 (2009).
- [39] R. Arnaldi et al. (NA60 Collaboration), *Eur. Phys. J. C* **64** 1 (2009).
- [40] G. Agakishiev et al. (HADES Collaboration), *Phys. Rev. C* **82**, 044907 (2010).
- [41] M.L. Benabderrahmane et al. (FOPI), *Phys. Rev. Lett.* **102**, 182501 (2009).
- [42] G. Agakishiev et al. (HADES Collaboration), *Phys. Rev. Lett* **103**, 132301 (2009).
- [43] A. Andronic, P. Braun-Munzinger, and K. Redlich, *Nucl. Phys. A* **765**, 211 (2006).
- [44] S. Wheaton, J. Cleymans, and M. Hauer, *Comput. Phys. Commun.* **180**, 84 (2009).
- [45] G. Agakishiev et al. (HADES Collaboration), *Eur. Phys. J. A* **47**, 21 (2011).
- [46] C. M. Ko et. al, *Phys. Rev. C* **85**, 064902 (2012).